ANTIOXIDANTS & REDOX SIGNALING
Volume 9, Number 10, 2007

DOI: 10.1089/ars.2007.1723

Forum Original Research Communication

High Spatial Resolution Multisite EPR Oximetry of Transient Focal Cerebral Ischemia in the Rat

BENJAMIN B. WILLIAMS, HUAGANG HOU, OLEG Y. GRINBERG, EUGENE DEMIDENKO, and HAROLD M. SWARTZ

ABSTRACT

***In vivo* electron paramagnetic resonance (EPR) spectroscopy can provide direct noninvasive, continuous, and repeatable measurements of oxygen in tissues. High-spatial-resolution multisite (HSRMS) oximetry is an EPR technique that uses applied magnetic field gradients to extend this capability to multiple implanted probes within the sample and accurately to estimate their respective local pO_2 values. These capabilities are crucial in experiments in which pO_2 varies across space and time and in which information about these variations is needed to describe physiologic and pathophysiologic phenomena and evaluate their responses to interventions such as therapy. One important application is the investigation of transient focal ischemia in the rat brain and the effects of treatment with hyperoxygenation. We used HSRMS oximetry with overmodulation to measure brain tissue oxygenation in a rat stroke model using lithium phthalocyanine as the oxygen probe. Oxygen measurements were made in a small cohort of rats at four implant sites during ischemia and reperfusion after transient focal ischemia initiated by occlusion of the middle cerebral artery. These measurements demonstrate the capabilities of the HSRMS oximetry technique and set the stage for more extensive physiologic studies.** *Antioxid. Redox Signal.* 9, 1691–1698.

INTRODUCTION

Several studies using the rat middle cerebral artery occlusion (MCAo) model have shown that hyperoxygenation introduced shortly after artery occlusion reduces infarct size substantially (1, 26, 28, 34, 37). While these studies demonstrate the potential for hyperoxygenation to treat cerebral ischemia, they do not include measurements of brain tissue po_2, the parameter that is most relevant for the rational development and evaluation of effective therapeutic schemes designed to increase brain oxygenation. In recognition of this need, a growing literature exists of studies using electron paramagnetic resonance (EPR) oximetry that provide such quantitative measurements of pO_2 in cerebral tissue and during ischemia in animal models (5, 9, 10, 13, 15–17, 21, 22).

In vivo EPR is a magnetic resonance technique that can be used to provide valuable physiologic information by using paramagnetic probes that have been implanted, injected, or generated in a research animal or human subject. Depending on the probe that is used, a wide range of information can be obtained with this technique, including tissue pO_2, pH, radiation exposure, and identification of free radical species (32). After the initial implantation or injection of the molecular probe, EPR measurements can be performed noninvasively. Tissue oxygenation can be directly measured through the broadening of the EPR absorption peaks of oxygen-sensitive paramagnetic materials that have been implanted or injected into the tissue (31). This technique has been used successfully in the study of oxygen concentration in various normal and pathologic tissues in rodents and rabbits (4, 9, 29, 30) and is now being devel-

Dartmouth EPR Center, Department of Radiology, Dartmouth Medical School, Hanover, New Hampshire.

oped for human applications, with feasibility studies under way in human subjects for repeated oximetry in solid cancers and peripheral vascular disease (11, 12, 33).

Numerous studies of cerebral tissue oxygenation have been performed using EPR with implanted paramagnetic probes in rodents, including measurements in rat models of stroke (5, 9, 10, 13, 15–17, 21, 22). The measurement of cerebral pO_2 with EPR oximetry is facilitated by the use of the oxygen sensitive paramagnetic probe lithium phthalocyanine (LiPc) (3, 14). Liu *et al*. (15–17) used EPR to study cerebral pO_2 in mice and rats with transient focal cerebral ischemia. In these studies, single implants of LiPc were placed in groups of animals at the expected locations of the core and penumbral regions of the infarct and in the contralateral hemisphere. Measurements at these regions were not acquired simultaneously in the same animals. Most recently, they demonstrated that the application of carbogen (95% O_2, 5% CO_2) for 90 min immediately after occlusion maintained normal pO_2 levels in the penumbral region of the infarct, reduced the infarct size, and improved neurologic function when compared with untreated controls (15). Hou *et al*. (27) used simultaneous multisite spectroscopy to measure pO_2 during a model of transient focal cerebral ischemia in rats (9). The brain tissue pO_2 was measured simultaneously at three separate sites where LiPc had been implanted. Two of the implants were in the ischemic hemisphere, at the expected locations of the core and penumbra of the ischemic region, with the remaining implant in the contralateral hemisphere. These measurements provided simultaneous pO_2 data throughout ischemia and reperfusion for these sites and enabled assessments of both local and global tissue oxygenation to be performed. By using this technique, simultaneous measurements at several sites were recorded, but the separation between the sites was limited to a minimum of 2.5 mm. High-spatial-resolution multisite (HSRMS) oximetry has the capability to provide similar measurements with an increased number of sites, the better to sample the ischemic volume and to provide more complete information.

The HSRMS EPR spectroscopy technique was developed to acquire high-spatial-resolution oximetry data quickly, with high precision and accuracy, at multiple sites simultaneously (6, 7, 27). HSRMS spectroscopy uses two consecutively acquired spectra with different magnetic field gradients and an analytic relation between these spectra to estimate accurately the intrinsic linewidths of multiple closely spaced implants or edges of single implants that are distributed spatially along one dimension. This relation applies to paramagnetic materials whose conventional CW EPR spectra are characterized by a single lorentzian peak and holds for each of the spatially separate regions in spectra acquired with a magnetic field gradient that are characterized by a uniform pO_2. The implant locations and magnetic field gradients must be chosen such that no overlap exists in the positions of the implants along the direction parallel to the gradient. As the EPR signals are effectively integrated over planes perpendicular to the gradient direction, the pO_2 within each plane is assumed to be uniform, and care should be taken in the experimental design to meet this assumption.

As described in the existing literature, the HSRMS technique is applicable only for spectra that have been acquired with modulation amplitudes low enough relative to the intrinsic linewidth that any broadening or distortion of the spectra is negligible. It has recently been recognized that the use of modulation amplitudes considerably larger than the intrinsic linewidth, referred to as overmodulation, can be used to increase the SNR of spectra for EPR imaging and to increase the precision of oximetry measurements (2, 20, 23, 36). Overmodulation can be used similarly with HSRMS spectroscopy if the applied modulation amplitudes are scaled in proportion with the magnitudes of the magnetic field gradients (35). The increase in SNR afforded by such overmodulation allows the measurements of implants deeper in tissue without unacceptable decreases in the precision of the oxygen measurements or increases in either the acquisition time or amount of implanted paramagnetic material.

MATERIALS AND METHODS

EPR spectroscopy

All EPR data were collected at L-band (~1.2 GHz) with a custom-built clinical spectrometer at Dartmouth Medical School (25). In these experiments, the spectrometer was equipped with a surface loop resonator with an automatic frequency-control system to mitigate the effects of animal motion on the recorded spectra (8, 24). The diameter of the detection loop was 8 mm. For HSRMS measurements, magnetic field gradients were generated by a pair of copper coils fixed in the Maxwell configuration. These air-cooled coils had a mean separation of 10.5 cm, 406 turns of 18-gauge wire each, and generated a gradient of 9 G/cm/A with modest increases in temperature.

LiPc preparation and calibration

All of these studies were performed with LiPc as the oxygen sensor. The LiPc was electrochemically synthesized at the EPR Center at Dartmouth Medical School following the published procedure (7). Calibration of the oxygen response in distilled water at physiologic temperature (37°C) showed a broadening of the peak-to-peak linewidth of 5.6 mG/mm Hg and an anoxic linewidth of 30 mG.

HSR-MS with overmodulation: phantom data

A set of experiments in a model system with uniform and stable pO_2 was performed to assess the ability of HSRMS to accurately and precisely estimate the pO_2 at multiple closely spaced sites. The phantom consisted of two groups of LiPc crystals similar in size and separation to those used for *in vivo* experiments, which were positioned in a sealed glass vial containing ~13 mm Hg O_2. Each group of crystals was ~50 μg, 1 mm in length, and 0.2 mm in diameter. The separation between the groups of crystal was 1.0 mm. Spectra without a magnetic field gradient were acquired with a range of modulation amplitudes (30 mG, 150 mG, and 294 mG) to measure the intrinsic linewidth of the oxygen probes in the sample and to verify the accuracy of the modulation amplitudes set by the spectrometer. The scan widths were 1 G for all spectra, and a scan time of 30 sec was used. The incident power was 0.4 mW, and saturation of the sample was negligible. The modulation frequency was held constant at a value of 27 kHz. These spectra

were analyzed by using spectral fitting with the model described by Robinson *et al*. (23), which is appropriate for lorentzian-shaped spectra.

The acquisition of these spectra was followed by several HSRMS experiments. For each experiment, five sets of spectra were acquired with gradient magnitudes of 4.75 G/cm and 9.31 G/cm. HSRMS data sets with the modulation amplitude set uniformly at 30 mG, 150 mG, and 294 mG were acquired, as was one dataset with modulation amplitudes set at 150 mG and 294 mG for the low- and high-gradient spectra, respectively. The scan widths were scaled in proportion to the gradient magnitudes and were 2.54 G and 4.98 G, respectively. Similarly, the scan times were 15 sec and 30 sec. All other acquisition parameters were the same as those used to acquire the zero-gradient spectra.

HSRMS during cerebral ischemia

Study design. Transient focal ischemia was initiated by a temporary occlusion of the middle cerebral artery in a cohort of eight male Sprague–Dawley rats (Charles River, MA) weighing between 250 and 310 g. Measurements of pO_2 in the expected penumbra region and in normal tissues in both the affected and contralateral hemisphere were made using HSRMS EPR oximetry. Measurements were made before, during, and immediately after the occlusion and also after 24 h of recovery in a subset of the rats. All animals were cared for according to the guidelines set by the National Institutes of Health, and the Institutional Animal Care and Use Committee of Dartmouth College reviewed and approved protocols for these animal experiments.

Implantation of LiPc. Implantation was performed 5–7 days before the experiment to allow the healing of any acute damage due to the procedure. Rats were anesthetized with an induction dose of 3.0–3.5% isoflurane at 1 L/min in 26% O_2, which was reduced to 2.0–2.5% for maintenance. Aggregates of LiPc crystals were implanted at four sites in the rat brain, three of which were in the ischemic (left) hemisphere, with the remaining site in the contralateral (right) hemisphere as a control. The implants were positioned to sample the penumbra and normal brain tissue based on prior knowledge of the approximate size and location of the infarction, according to the surgical design and cerebrovascular architecture (18) and as revealed by TTC staining performed earlier in similar experiments (5, 9). The penumbra is that region that remains viable shortly after ischemia, but later develops into nonviable tissue. For each rat, all of the sites were located at a uniform distance of either 0.5 or 2.0 mm posterior to the bregma and were placed at distinct nonoverlapping positions along the medial–lateral axis of the rat. Two of the sites in the ischemic hemisphere were chosen to have a high likelihood of sampling the penumbra. These were the lateral implant, positioned 4.5 mm from the midline at a depth of 1.5 mm, and a deep implant placed 3.0 mm from the midline at a depth of 4.0 mm. The remaining two implants were intended to sample normal tissue and were placed 1.5 mm on either side of the midline at a depth of 1.5 mm. These implant positions are shown in Fig. 1. Holes were drilled through the skull directly above the implant sites, and 50–80 μg of LiPc was deposited at each site by using either a 23- or 25-gauge needle/trocar combination. Precise positioning of the implants was achieved through the use of an MM-4100 Stereotaxic Micromanipulator (ASI Instruments, Inc., Warren, MI), which features adjustments with 50-μm readability along three axes of motion. Before implantation, the needle was loaded with the LiPc crystals, and the trocar was inserted but not advanced within the needle. By using the stereotaxic device, the needle was positioned above the intended implant site and advanced into the brain tissue to the desired depth. The needle was then retracted 0.5 mm, and the LiPc was implanted by advancing the trocar so that its tip was at the same depth as the tip of the needle.

MCAo model. Throughout the measurements and surgeries, the rats were continuously anesthetized by using inspired isoflurane in a mixture with 26% O_2 at a flow rate of 1 L/min. For the induction of anesthesia, 3–4% isoflurane was applied. Surgery was performed with 2–2.5% isoflurane, and the main-

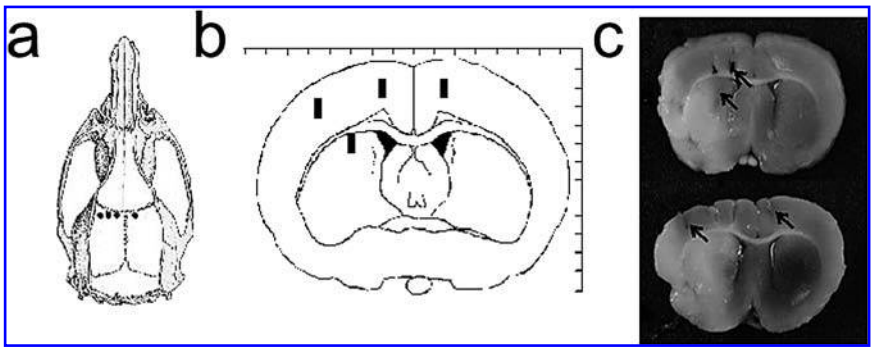

FIG. 1. Anatomic positions of the LiPc implants and focal ischemia. These diagrams show the locations of the LiPc implants in (**a**) the view from the top of the skull and (**b**) a coronal slice through the rat brain. Physical examination of slices through the brain during necropsy confirmed that the positioning of the LiPc implants was accurate and reproducible. The images in panel (**c**) show photographs of the TTC-stained tissue containing the implants for a single rat. A cut was made along the plane defined by the LiPc implants, and the crystals are found near the opposing surfaces of the two neighboring 2-mm slices. The locations of the implants are identifiable, although the deep implant in the ischemic hemisphere is partially occluded by tissue. The differentiation between the darkly stained normal tissue and lighter unstained region where the ischemia has led to cell damage and death is apparent.

tenance dose used during EPR measurements was 1.2–1.5%. Core body temperature was monitored by using a rectal-probe thermometer and kept in the normal physiologic range by using a combination of heat lamps, a warm-water blanket, and the flow of warm air over the rat's body.

Directly after a series of baseline HSRMS oximetry measurements, the rat was removed from the magnet, and the MCAo surgery was performed. Transient focal cerebral ischemia was induced by the intraluminal suture MCAo method, as previously described (5, 9, 18). After the MCAo surgery, the rat was returned to the magnet for another series of pO_2 measurements taken over the next 2 h with the occlusion intact. This was followed by surgery to reverse the occlusion and then a third series of pO_2 measurements during the reperfusion period. A subset of the animals was kept overnight, and sets of pO_2 measurements were performed ~24 h after the initiation of the occlusion. After final measurements, rats were immediately killed, and the brains were isolated for gross histologic analysis and staining with 2% 2′,3′,5′-triphenyl-2H-tetrazolium chloride (TTC). This staining distinguishes between viable cells with mitochondrial dehydrogenase activity and those cells that have been damaged or killed by the ischemia and therefore lack this activity.

Data acquisition

HSRMS spectra at each gradient magnitude were acquired in a scan-by-scan alternating pattern and separately recorded. This alternating pattern was used to guard against any bias between the high- and low-gradient spectra due to potential changes in instrumental or physiologic conditions during the acquisition. Typically, five or six spectra were collected at each gradient magnitude and averaged to increase the signal-to-noise ratio. These spectra were acquired using similar instrumental settings to those used in the phantom studies. The scan range and scan times were doubled to reflect the larger size of this implant distribution. The incident RF power was set to avoid saturation and varied between 12 and 40 mW. With these parameters, complete sets of HSRMS data were each acquired in 7.5 min.

Data analysis

The analysis of the HSRMS oximetry data was performed with software written for Matlab (The Mathworks, Natick MA). A graphic user interface displays the averaged low- and high-gradient spectra and allows the user to define manually the separate fitting regions for each of the implant sites. For HSRMS estimation of the intrinsic linewidth at each site, the software convolves the high-gradient spectrum with a lorentzian distribution and varies the width of this lorentzian to minimize the least-squared error between the result of the convolution and the low-gradient spectrum within the region of interest. The phase, field center, and intensity of the lorentzian distribution were set to reflect no changes in these parameters between the high- and low-gradient spectra. The width of this lorentzian distribution is equal to $\frac{\Gamma}{G_1} - \frac{\Gamma}{G_2}$, where Γ is the intrinsic oxygen-dependent linewidth of the implanted material at that location, and G_1 and G_2 are the low- and high-gradient magnitudes, respectively. After solving for Γ, the oxygen calibration for the LiPc is used to estimate the pO_2.

RESULTS

Evaluation of phantom measurements

Analyses of the spectra collected without gradients were performed, and the resultant linewidth estimates were consistent to within an acceptable level of instrumental error. The SNR values ranged from 13 for the spectra with 30 mG modulation amplitude up to near 60 for the overmodulated spectra. The peak-to-peak linewidth for spectra collected with the low-modulation amplitude of 30 mG was estimated to be 104.0 ± 0.7 mG. When the modulation amplitude was increased to 150 and 294 mG, the linewidth estimates were 104.4 ± 0.2 and 105.1 ± 0.3 mG, respectively. This consistency confirms the accuracy of the set modulation amplitudes. Single scans from these spectra and their fits and residuals are shown in Fig. 2. In each case, the residuals are largely devoid of structure, indicating that the fits were satisfactory.

HSRMS analysis was performed on the data sets collected with uniform modulation amplitudes of 30, 150, and 294 mG. With 30 mG modulation, where associated broadening is negligible, linewidths for the left and right groups of crystals estimated from single scans were 115 ± 19 and 101 ± 26 mG. The SNR values in these spectra were ~5. When higher-modulation amplitudes were used uniformly for both spectra, the distortion in the spectra prohibited accurate estimation of the intrinsic linewidths, and large residuals were invariably observed. In these spectra, the SNR was ~20. When the larger-modulation amplitudes were used, but scaled in proportion to the applied gradient magnitudes, the estimated linewidths were 110 ± 1 and 101 ± 2 mG. These values are both within 1 mm Hg of the value measured from the bulk sample without gradients. Figure 3 shows the low-gradient spectra for examples from the 30 mG and proportionately overmodulated data sets, the HSRMS fits for each site, and the pO_2 estimates.

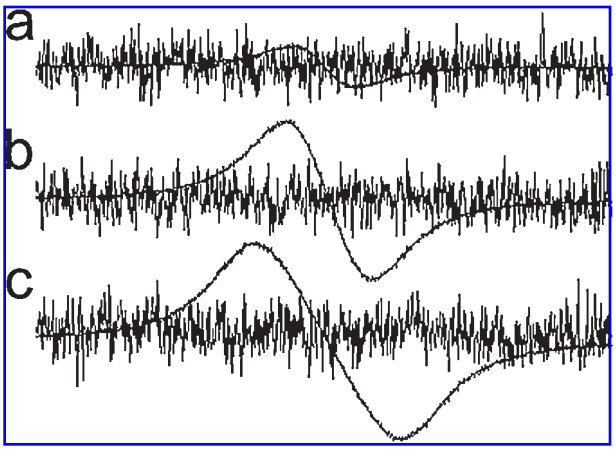

FIG. 2. Zero-gradient LiPc spectra with overmodulation and spectral fitting. Spectra were acquired of the multisite LiPc phantom (intrinsic peak-to-peak linewidth, 104 mG) without magnetic field gradients at modulation amplitudes of (**a**) 30 mG, (**b**) 150 mG, and (**c**) 294 mG. All spectra are shown on the same scale, with the fitted spectrum overlaid, and the residual shown with ×10 magnification. In each case, spectral fitting accurately estimated the intrinsic linewidth.

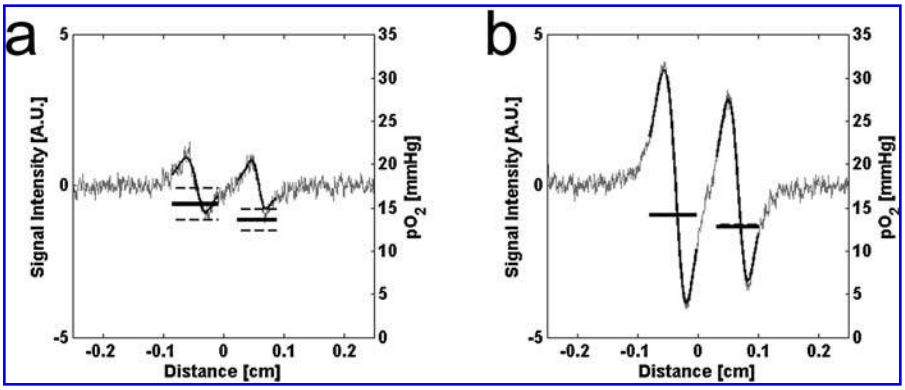

FIG. 3. HSRMS analysis of multisite LiPc phantom. HSRMS oximetry was applied to measure the pO_2 at both sites in the multisite phantom with (**a**) conventional low modulation (30 mG for both spectra) and (**b**) overmodulation (150 mG with the lower gradient and 294 mG with the higher gradient). Each plot shows the spatially registered EPR signal intensity and fit to these data (left ordinate), as well as the pO_2 values estimated for each site (right ordinate). Accurate pO_2 values were estimated under both sets of conditions, but the standard error of the pO_2 estimate decreased by a factor of ~15 with overmodulation.

Infarct region. Inspection of the TTC-stained slices showed that the LiPc implants were located in the intended anatomic positions and that the MCAo surgery had caused ischemia, leading to cell damage and cell death in each rat. Figure 1c shows a typical set of such slices. In each rat, the locus of the infarct region was in the subcortex ~5 mm from the midline at a depth of 5 mm. After 2 h of occlusion and 22 h of reperfusion, the infarct region encompassed the majority of the subcortex and the lateral half of the cortex in the ischemic hemisphere. The lateral and deep implants were located along the edge of this region in the penumbra, and the other two implants remained in viable tissue.

HSRMS oximetry. The pO_2 estimates were made throughout the experimental periods using the HSRMS method for each of the sites in each of the rats. Figure 4 shows experimental data and the fitting results for three time points for a typical animal. Low-gradient spectra from the baseline, occlusion, and reperfusion periods are shown in gray, with the results of the HSRMS fitting superimposed in black. Also included are the pO_2 values, with errors, estimated for each region and time point. The EPR signals from all four of the implants are clearly distinguishable in each spectrum. The signals from the implants in the ischemic hemisphere are on the left, or low-field, side of each spectrum, and the contralateral implant signal is to the right. In these spectra, the SNR varied from ~6, for the deep site and the contralateral site in the occlusion spectrum where the B_1 amplitude is low, up to values >20 for the medial site in the ischemic hemisphere. The effect of the occlusion on the pO_2 at the deep site is especially apparent. As the estimated pO_2 decreases from 18.4 ± 1.1 mm Hg during baseline to 7.4 ± 0.5 mm Hg during ischemia, the linewidth decreases, and the amplitude of the signal increases markedly.

Baseline pO_2 values varied considerably from site to site and from rat to rat. The mean pO_2 over all sites and all rats was 25 ± 9 mm Hg. Because of these differences, the change in pO_2 relative to the baseline value was calculated for each site in

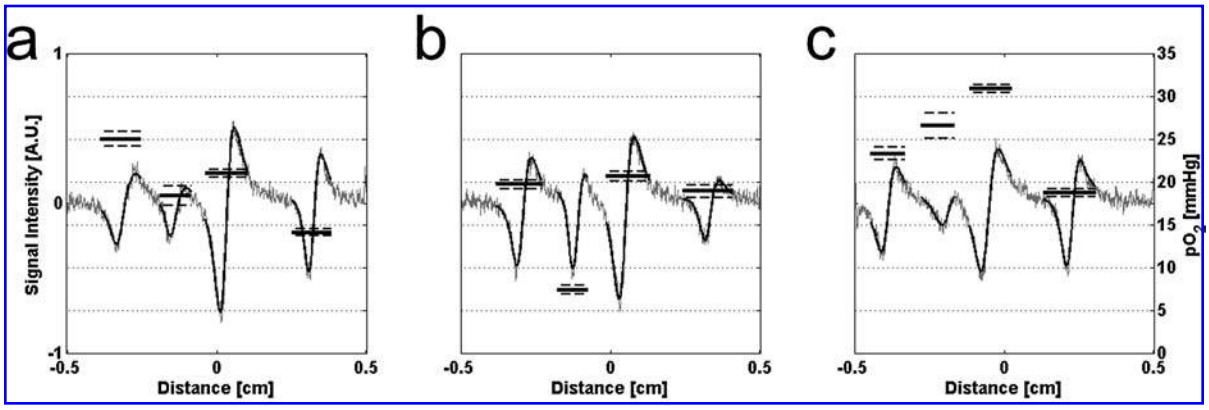

FIG. 4. HSRMS Analysis of *in vivo* data during transient focal ischemia. Shown in this panel are low-gradient spectra recorded during the (**a**) baseline, (**b**) occlusion, and (**c**) reperfusion periods for a single rat. Each spectrum is an average of five 30–sec scans acquired over a period of 7.5 min. All spectra are shown on the same scale. Each plot shows the spatially registered EPR signal intensity and fit to these data (left ordinate), as well as the pO_2 values estimated for each site (right ordinate).The high-gradient spectra used in the HSRMS analyses are not shown.

each rat. For the same experiment described in Fig. 4, the changes in pO_2 relative to the mean baseline pO_2 for each site during the baseline, occlusion, and reperfusion periods are shown in Fig. 5. The pO_2 at the sites of the lateral and deep implants in the ischemic hemisphere are observed to drop >10 mm Hg from their baseline values. These data show that the pO_2 does not fall uniformly at these sites, but rather that the pO_2 change at the lateral site lags >45 min behind that at the deep site for this rat. For the medial sites in both hemispheres the pO_2 is observed to vary closely about baseline values during occlusion. On reperfusion, the pO_2 at each of the sites in the ischemic hemisphere increases relative to the value during the occlusion, and the pO_2 at the deep site is observed to rebound >10 mm Hg beyond its baseline value. The pO_2 at the contralateral site does not change significantly between occlusion and reperfusion.

Similar results were observed for each of the other rats in this study, although variation in the sizes of the infarct regions led to significant variability among the pO_2 measurements at each site. Figure 6 shows the changes in pO_2 for each of the four sites and experimental periods, averaged across rats and time. Despite the variability due to infarct sizes, trends in the data are observed. At the lateral and deep sites in the ischemic hemisphere, which are intended to sample the periphery of the infarct region, decreases in the pO_2 were observed. The pO_2 at these same sites was observed to rebound to baseline levels during reperfusion and then vary considerably after 24 h of recovery. The medial sites in both hemispheres showed much less variation, which may be expected, as they are distant from the focal ischemia.

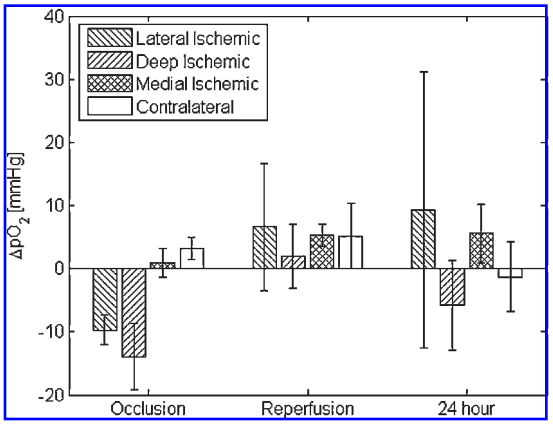

FIG. 6. Mean pO_2 measurements across rats. The average changes in pO_2 from baseline for each of the implant sites during occlusion, reperfusion, and at 24 h after occlusion are shown. Each shaded bar denotes the mean pO_2 for a given site, and error bars denote the standard error. The deep and lateral sites in the ischemic hemisphere report reduced pO_2 during occlusion and a rebound to near-baseline values during reperfusion. (Occlusion, $n = 6$; reperfusion, $n = 4$; 24-h, $n = 3$).

DISCUSSION

The development of these techniques lays the groundwork for subsequent studies, in which monitoring of cerebral pO_2 throughout the duration of a stroke could be used to evaluate and optimize treatment protocols. The power of this technique lies in its ability simultaneously to measure pO_2 at multiple closely spaced sites throughout the duration of the stroke model from baseline to recovery. Through such measurements, the changes in pO_2 at specific locations relative to the infarct can be measured and the relations between the pO_2 values at different sites can be assessed. This will allow investigation of the temporal changes in the size of the ischemic region and severity of ischemia after occlusion and allow therapeutic techniques to be evaluated.

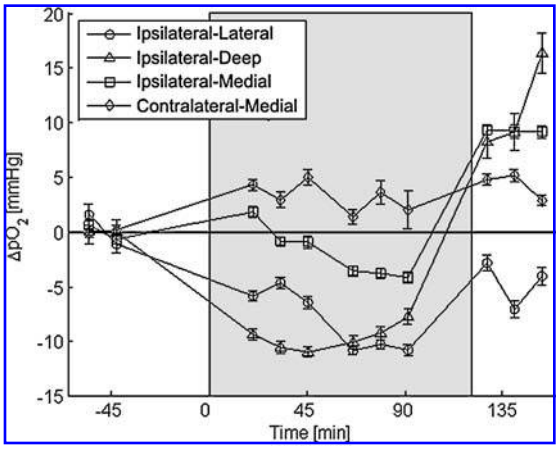

FIG. 5. Dynamic pO_2 measurements during cerebral ischemia/. HSRMS oximetry allows the simultaneous measurement of pO_2 at each of the implant sites throughout the course of the experiment. Shown here is an example of the changes in pO_2 from baseline observed during occlusion and reperfusion. The 120–min period of occlusion is shaded. During this period, the lateral and deep sites in the ischemic hemisphere are acutely affected, and the pO_2 at these locations decreases >10 mm Hg, although not at the same rate.

In the animal studies, a large amount of variation in the baseline pO_2 values was observed from site to site within a single rat and also across rats. The mean pO_2 value found across all rats and all sites (25 ± 9 mm Hg) is slightly smaller than, but not inconsistent with, those of similar previous studies (9, 16, 17), which reported mean pO_2 values between 30 and 35 mm Hg. Differences in the pO_2 values between sites may be representative of heterogeneity of the oxygen in brain tissue. Significant heterogeneity in cerebral pO_2 in rats has been reported in previous studies in which measurements were performed using EPR oximetry, polarographic oximetry with the Eppendorf electrode, and the Oxylite system (Oxford Optronix, Oxford, U.K.) (19, 21, 22). O'Hara *et al*. (21, 22) reported that significant pO_2 heterogeneity was found with each method, with standard deviations of greater than 20% of the mean pO_2 values. ANOVA was applied to characterize the variance of the pO_2 measurements made with EPR oximetry, and the total variance of the pO_2 measurements was attributed to between-animal and spatial variance, rather than to variance associated with the measurement technique (22). Lübbers and Baumgärtl (19) used a polarographic needle electrode to measure pO_2 profiles within the rat cerebral cortex and reported a heterogeneous distribution, with values ranging from 5 to 85 mm Hg. Despite the large variation among individual baseline pO_2 measurements in the

current study, no statistically significant differences from the overall mean value were found between any of the rats or sites. In these experiments, the core temperatures of the rats were maintained within the normal physiologic range, but the blood pressure and end-tidal CO_2 were not monitored, and the rats were not ventilated. It is possible that reduced blood pressure or increased $paCO_2$ in these studies led to a general reduction in blood flow and brain-tissue oxygenation.

A second difficulty encountered in this study was the variability in the sizes of the regions affected by the infarct. Based on prior reports in the literature and the use, in this case, of a surgeon with extensive successful experience with this model, it is reasonable to conclude that the variability is due to the intrinsic nature of the model. Because of this variability, the relations between the implant sites and the ischemia were not uniform across rats, and the *a priori* assignment of implant sites to the core or periphery of the infarct region is not ideal. Even with consistent positioning of the LiPc implants, this variability brings into question the appropriateness of averaging results across a cohort of rats. However, some type of pooling is necessary to obtain statistically significant results and proper evaluation of therapeutic measures. One feasible approach would be to characterize the positions of individual implants with respect to the infarct based on postmortem anatomic analysis and then to use data based on this characterization, rather than on absolute position, in the analysis of general results.

CONCLUSIONS

In this study of cerebral ischemia and reperfusion, the HSRMS technique demonstrated the ability to measure pO_2 simultaneously at several sites near the focus of the infarct. The HSRMS technique allows the use of several closely spaced implants to measure multiple points within the ischemic regions and thereby gain high-resolution information about the development of the infarct. Such data can be used to characterize the development of the ischemic region over space and time, and the effects of therapeutic measures.

ACKNOWLEDGMENTS

This work was supported by a grant from the GEMI Fund (Linde Gas Therapeutics, Lindingö, Sweden) and used the facilities of NIH grant P41 EB002032, "EPR Center for the Study of Viable Systems."

ABBREVIATIONS

CW, continuous wave; EPR, electron paramagnetic resonance; HSRMS, high-spatial-resolution multisite; HWHM, half width, half maximum; LiPc, lithium phthalocyanine; MCAo, middle cerebral artery occlusion; RF, radiofrequency; SNR, signal-to-noise ratio; TTC, 2% 2′,3′,5′-triphenyl-2H-tetrazolium chloride.

REFERENCES

1. Chang CF, Niu KC, Hoffer BJ, Wang Y, and Borlongan CV. Hyperbaric oxygen therapy for treatment of postischemic stroke in adult rats. *Exp Neurol* 166: 298–306, 2000.
2. Deng Y, Pandian RP, Ahmad R, Kuppusamy P, and Zweier JL. Application of magnetic field over-modulation for improved EPR linewidth measurements using probes with lorentzian lineshape. *J Magn Reson* 181: 254–261, 2006.
3. Dunn JF and Swartz HM. In vivo electron paramagnetic resonance oximetry with particulate materials. *Methods* 30: 159–166, 2003.
4. Grinberg OY, Hou H, Grinberg SA, Moodie KL, Demidenko E, Friedman BJ, Post MJ, and Swartz HM. Po2 and regional blood flow in a rabbit model of limb ischemia. *Physiol Measure* 25: 659, 2004.
5. Grinberg OY, Hou H, and Swartz HM. Direct repeated measurements of po_2 in the brain during ischemia and reperfusion, ischemic blood flow in the brain. In: *Keio university symposia for life science and medicine*, edited by Fukuuchi Y, Tomita M, and Koto A. Tokyo: Springer-Verlag, 2000, pp. 381–389.
6. Grinberg OY, Smirnov AI, and Swartz HM. High spatial resolution multi-site EPR oximetry. *J Magn Reson* 152: 247–258, 2001.
7. Grinberg VO, Smirnov AI, Grinberg OY, Grinberg SA, O'Hara JA, and Swartz HM. Practical experimental conditions and limitations for high-spatial-resolution multisite EPR oximetry. *Appl Magn Reson* 28: 69–78, 2005.
8. Hirata H, Walczak T, and Swartz HM. Electronically tunable surface-coil-type resonator for l-band EPR spectroscopy. *J Magn Reson* 142: 159–167, 2000.
9. Hou H, Grinberg O, Grinberg S, and Swartz H. Cerebral tissue oxygenation in reversible focal ischemia in rats: multi-site EPR oximetry measurements. *Physiol Meas* 26: 131–141, 2005.
10. Hou H, Grinberg OY, Taie S, Leichtweis S, Miyake M, Grinberg S, Xie H, Csete M, and Swartz HM. Electron paramagnetic resonance assessment of brain tissue oxygen tension in anesthetized rats. *Anesth Analg* 96: 1467–1472, 2003.
11. Khan N, Williams BB, Hou H, Li H, and Swartz HM. Repetitive tissue po_2 measurements by electron paramagnetic resonance oximetry: current status and future potential for experimental and clinical studies. *Antioxidant Redox Signal* 2006 (in press).
12. Khan N, Williams BB, and Swartz HM. Clinical applications of in vivo EPR: rationale and initial results. *Appl Magn Reson* 30: 185–199, 2006.
13. Liu KJ, Bacic G, Hoopes PJ, Jiang J, Du H, Ou LC, Dunn JF, and Swartz HM. Assessment of cerebral po_2 by EPR oximetry in rodents: effects of anesthesia, ischemia, and breathing gas. *Brain Res* 685: 91–98, 1995.
14. Liu KJ, Gast P, Moussavi M, Norby SW, Vahidi N, Walczak T, Wu M, and Swartz HM. Lithium phthalocyanine: a probe for electron paramagnetic resonance oximetry in viable biological systems. *Proc Natl Acad Sci U S A* 90: 5438–5442, 1993.
15. Liu S, Liu W, Ding W, Miyake M, Rosenberg GA, and Liu KJ. Electron paramagnetic resonance-guided normobaric hyperoxia treatment protects the brain by maintaining penumbral oxygenation in a rat model of transient focal cerebral ischemia. *J Cereb Blood Flow Metab* 26: 1274–1284, 2006.
16. Liu S, Shi H, Liu W, Furuichi T, Timmins GS, and Liu KJ. Interstitial po_2 in ischemic penumbra and core are differentially affected following transient focal cerebral ischemia in rats. *J Cereb Blood Flow Metab* 24: 343–349, 2004.
17. Liu S, Timmins GS, Shi H, Gasparovic CM, and Liu KJ. Application of in vivo EPR in brain research: monitoring tissue oxygenation, blood flow, and oxidative stress. *NMR Biomed* 17: 327–334, 2004.
18. Longa EZ, Weinstein PR, Carlson S, and Cummins R. Reversible middle cerebral artery occlusion without craniectomy in rats. *Stroke* 20: 84–91, 1989.
19. Lubbers DW and Baumgartl H. Heterogeneities and profiles of oxygen pressure in brain and kidney as examples of the po_2 distribution in the living tissue. *Kidney Int* 51: 372–380, 1997.
20. Mailer C, Robinson BH, Williams BB, and Halpern HJ. Spectral fitting: the extraction of crucial information from a spectrum and a spectral image. *Magn Reson Med* 49: 1175–1180, 2003.

21. O'Hara JA, Hou H, Demidenko E, Springett RJ, Khan N, and Swartz HM. Simultaneous measurement of rat brain cortex pto_2 using EPR oximetry and a fluorescence fiber-optic sensor during normoxia and hyperoxia. *Physiol Meas* 26: 203–213, 2005.
22. O'Hara JA, Khan N, Hou H, Wilmo CM, Demidenko E, Dunn JF, and Swartz HM. Comparison of EPR oximetry and Eppendorf polarographic electrode assessments of rat brain pto_2. *Physiol Meas* 25: 1413–1423, 2004.
23. Robinson BH, Mailer C, and Reese AW. Linewidth analysis of spin labels in liquids, I: theory and data analysis. *J Magn Reson* 138: 199–209, 1999.
24. Salikhov I, Hirata H, Walczak T, and Swartz HM. An improved external loop resonator for in vivo L-band EPR spectroscopy. *J Magn Reson* 164: 54–59, 2003.
25. Salikhov I, Walczak T, Lesniewski P, Khan N, Iwasaki A, Comi R, Buckey J, and Swartz HM. EPR spectrometer for clinical applications. *Magn Reson Med* 54: 1317–1320, 2005.
26. Schabitz WR, Schade H, Heiland S, Kollmar R, Bardutzky J, Henninger N, Muller H, Carl U, Toyokuni S, Sommer C, and Schwab S. Neuroprotection by hyperbaric oxygenation after experimental focal cerebral ischemia monitored by MRI. *Stroke* 35: 1175–1179, 2004.
27. Smirnov AI, Norby SW, Clarkson RB, Walczak T, and Swartz HM. Simultaneous multi-site EPR spectroscopy in vivo. *Magn Reson Med Official J Soc Magn Reson Med* 30: 213–220, 1993.
28. Sunami K, Takeda Y, Hashimoto M, and Hirakawa M. Hyperbaric oxygen reduces infarct volume in rats by increasing oxygen supply to the ischemic periphery. *Crit Care Med* 28: 2831–2836, 2000.
29. Swartz HM. The measurement of oxygen in vivo using EPR techniques. In: *Biological Magnetic Resonance*. Vol 20: *In Vivo EPR (ESR): Theory and Applications*, edited by Berliner LJ. New York: Plenum Publishing, 2002, pp. 404–440.
30. Swartz HM. Using EPR to measure a critical but often unmeasured component of oxidative damage: oxygen. *Antioxid Redox Signal* 6: 677–686, 2004.
31. Swartz HM and Clarkson RB. The measurement of oxygen in vivo using EPR techniques. *Phys Med Biol* 43: 1957–1975, 1998.
32. Swartz HM and Halpern H. EPR studies of living animals and related model systems (in vivo EPR). *Biol Magn Reson* 14: 367–404, 1998.
33. Swartz HM, Khan N, Buckey J, Comi R, Gould L, Grinberg O, Hartford A, Hopf H, Hou H, Hug E, Iwasaki A, Lesniewski P, Salikhov I, and Walczak T. Clinical applications of EPR: overview and perspectives. *NMR Biomed* 17: 335–351, 2004.
34. Veltkamp R, Warner DS, Domoki F, Brinkhous AD, Toole JF, and Busija DW. Hyperbaric oxygen decreases infarct size and behavioral deficit after transient focal cerebral ischemia in rats. *Brain Res* 853: 68–73, 2000.
35. Williams BB, Grinberg OY, Demidenko E, and Swartz HM. Resolution of heterogeneity of oxygen in tissues using EPR oximetry with particulates: high spatial resolution multi-site oximetry with overmodulation. In: Proceedings of 12th Annual Meeting of ISMRM, Kyoto, Japan: 2256, 2004.
36. Williams BB, Pan X, and Halpern HJ. Epr imaging: the relationship between CW spectra acquired from an extended sample subjected to fixed stepped gradients and the radon transform of the resonance density. *J Magn Reson* 174: 88–96, 2005.
37. Yang ZJ, Camporesi C, Yang X, Wang J, Bosco G, Lok J, Gorji R, Schelper RL, and Camporesi EM. Hyperbaric oxygenation mitigates focal cerebral injury and reduces striatal dopamine release in a rat model of transient middle cerebral artery occlusion. *Eur J Appl Physiol* 87: 101–107, 2002.

Address reprint requests to:
Benjamin B. Williams
Department of Radiology
Hinman Box 7785
Hanover, NH 03755

E-mail: ben.williams@dartmouth.edu

Date of first submission to ARS Central, April 27, 2007; date of final revised submission, May 17, 2007; date of acceptance, May 21, 2007.

This article has been cited by:

1. Nadeem Khan, Sriram Mupparaju, Huagang Hou, Benjamin B. Williams, Harold Swartz. 2011. Repeated assessment of orthotopic glioma pO2 by multi-site EPR oximetry: A technique with the potential to guide therapeutic optimization by repeated measurements of oxygen. *Journal of Neuroscience Methods* . [CrossRef]
2. R. Ahmad, S. Som, D.H. Johnson, J.L. Zweier, P. Kuppusamy, L.C. Potter. 2011. Multisite EPR oximetry from multiple quadrature harmonics. *Journal of Magnetic Resonance* . [CrossRef]
3. Reut Avni, Batya Cohen, Michal Neeman. 2011. Hypoxic stress and cancer: imaging the axis of evil in tumor metastasis. *NMR in Biomedicine* n/a-n/a. [CrossRef]
4. R. Ahmad, G. Caia, L.C. Potter, S. Petryakov, P. Kuppusamy, J.L. Zweier. 2010. In vivo multisite oximetry using EPR–NMR coimaging. *Journal of Magnetic Resonance* **207**:1, 69-77. [CrossRef]
5. Nadeem Khan, Sriram Mupparaju, Shahryar K. Hekmatyar, Huagang Hou, Jean P. Lariviere, Eugene Demidenko, David J. Gladstone, Risto A. Kauppinen, Harold M. Swartz. 2010. Effect of Hyperoxygenation on Tissue pO2 and Its Effect on Radiotherapeutic Efficacy of Orthotopic F98 Gliomas. *International Journal of Radiation Oncology*Biology*Physics* **78**:4, 1193-1200. [CrossRef]
6. Nadeem Khan , Valery V. Khramtsov , Harold M. Swartz Methods for Tissue pO2, Redox, pH, and Glutathione Measurements by EPR Spectroscopy 81-89. [Abstract] [Summary] [PDF] [PDF Plus]
7. Nadeem Khan, Hongbin Li, Huagang Hou, Jean P. Lariviere, David J. Gladstone, Eugene Demidenko, Harold M. Swartz. 2009. Tissue pO2 of Orthotopic 9L and C6 Gliomas and Tumor-Specific Response to Radiotherapy and Hyperoxygenation. *International Journal of Radiation OncologyBiologyPhysics* **73**:3, 878-885. [CrossRef]
8. Dipak K. Das Methods in Redox Signaling . [Citation] [Full Text] [PDF] [PDF Plus]